THE ASTROPHYSICAL JOURNAL, 453:673–684, 1995 November 10

THE MULTIPHASE STRUCTURE OF THE GALACTIC HALO: HIGH-VELOCITY CLOUDS IN A HOT CORONA

MARK G. WOLFIRE,[1] CHRISTOPHER F. MCKEE,[2] DAVID HOLLENBACH,[3] AND A. G. G. M. TIELENS[3]
Received 1995 March 8; accepted 1995 May 18

ABSTRACT

Observations indicate that some high-velocity clouds (HVCs) have a two-phase structure consisting of cold cores and warm envelopes. We calculate the thermal equilibrium gas temperature and investigate the thermal stability of neutral gas in the Galactic halo. Phase diagrams (thermal pressure P vs. gas density n) are presented for gas at a range of heights z above the Galactic plane. Our method accounts for the photoelectric heating from small grains and PAHs and includes a detailed treatment of the ionization rates and heating due to the soft X-ray background and due to cosmic rays. We find that stable two-phase gas exists over a range of heights, but only within a narrow range of pressures at each height. Using a realistic Galactic gravitational potential and using halo parameters consistent with observed properties of the soft X-ray background, we show that a hot ($T \sim 1$–2×10^6 K) Galactic corona can provide the necessary pressure for two-phase HVCs.

We find that for an isothermal $T = 10^6$ K halo, the observed X-ray emission measure ($EM_h = 2.5 \times 10^{-3}$ pc cm^{-6}) yields a thermal pressure in the Galactic midplane of $\simeq 2000$–3000 K cm^{-3}, similar to observed pressures. In addition, we find that the electrons in the hot halo make a nonnegligible contribution to the dispersion measure of pulsars far from the Galactic plane. A method is presented for estimating HVC distances from X-ray shadowing measurements.

We demonstrate that the two-phase nature of HVCs can be used to constrain the distance to the clouds and their metallicity or origin. A primordial origin (extremely low metallicities) can be ruled out since two phases exist only for $z < 2$ kpc, contrary to most distance lower limits to HVCs. An extragalactic origin for some clouds, a result of gas stripped from the LMC, is supported by our calculated range of distances over which two-phase clouds exist in a hot corona, the observed dust and metal content, and the high velocities observed for a few HVCs. We predict that no cold cores are expected to be found in a $T = 10^6$ K halo at distances greater than ~ 20 kpc, which is consistent with the lack of cold cores seen in the Magellanic Stream. However, the mass infall rate to the Galactic plane, and the general velocity distribution of halo clouds is consistent with an origin from gas injected into the halo by a Galactic fountain. For this case, two-phase models require that the abundance of very small grains and PAHs in the fountain clouds must be similar to the standard abundances in the disk.

Subject headings: Galaxy: halo — ISM: clouds — ISM: structure

1. INTRODUCTION

High-velocity clouds (HVCs) are neutral hydrogen clouds with velocities which exceed $|v_{lsr}| > 100$ km s^{-1} and are incompatible with simple Galactic rotation. Several models for the origin of HVCs have been proposed, including cloud condensation in a Galactic fountain driven by supernovae explosions (Shapiro & Field 1976; Bregman 1980; Corbelli & Salpeter 1988; Houck & Bregman 1990; Li & Ikeuchi 1992; Rosen & Bregman 1995), stripped LMC gas (Mathewson, Cleary, & Murray 1974; Giovanelli 1980, 1981), and infalling primordial gas (Oort 1966, 1970; see also Wakker 1989, chap. 5, and review by Wakker 1991a). Surveys of high-velocity gas reveal several groups or "complexes" of clouds lying close together in position and velocity (Bajaja et al. 1985; Hulsbosch & Wakker 1988; Wakker & van Woerden 1991). At least one complex may be explained by a high-z extension of an outer Galactic spiral arm (Habing 1966; Kepner 1970), while another is associated with the Magellanic Stream—gas either tidally (Murai & Fujimoto 1980; Lin, Jones, & Klemola 1995) or ram pressure stripped (Moore & Davis 1994) from the Magellanic Clouds. The majority of complexes, however, are not simply associated with known Galactic or extragalactic counterparts.

The origin of HVCs is unresolved in part because the metallicity and distance is known or bracketed for only a few clouds. The metal abundance has been estimated from the detection of metal absorption lines at ultraviolet and optical wavelengths toward HVCs with bright background sources (e.g., Savage & de Boer 1979, 1981; West et al. 1985; Robertson et al. 1991; Bowen & Blades 1993). Savage et al. (1993) report *HST* observations toward three quasars with lower limits to the gas phase Mg abundance ranging from 0.056 to 0.3 times solar. Recent observations of several clouds associated with the Magellanic Stream indicate metallicities derived from sulfur abundances $\lesssim 0.30$ times solar (Lu, Savage, & Sembach 1994b). In addition, Lu, Savage, & Sembach (1994a) report sulfur abundances of ~ 0.15 times solar for one of the extreme positive velocity clouds located on the sky opposite the Magellanic Stream and beyond the Magellanic Clouds. This HVC may be part of a population stripped from a Local Group object (either the Magellanic Clouds or another member of the Local Group; Lynden-Bell 1976; West et al. 1985; Lu et al. 1994a). The sulfur observations, in particular, are significant because of the low depletions expected for S in the diffuse gas. Sembach et

[1] Department of Astronomy, University of California at Berkeley. Postal address: Laboratory for Astrophysics, National Air and Space Museum, Smithsonian Institution, Washington, DC 20560.
[2] Physics Department, and Astronomy Department, University of California at Berkeley, Berkeley, CA 94720.
[3] NASA Ames Research Center, MS 245-3, Moffett Field, CA 94035.

al. (1995) have discovered a highly ionized, low H I column density [$N(\mathrm{H\ I}) < 5 \times 10^{17}$ cm^{-2}] high-velocity cloud with abundances estimated at between 0.06 and 0.2 times solar. Meyer & Roth (1991) also reported Ca II absorption in an HVC with no detectable H I 21 cm emission indicating a very low H I column. The evidence suggests, at least for the few lines of sight available, that the metallicity is greater than primordial but less than solar.

A search for dust in HVCs was carried out by Wakker & Boulanger (1986) who searched for, but did not detect, *IRAS* emission toward two directions in complex A and one direction in complex M. They demonstrate that these clouds must be either at great distances from the Galactic plane ($z > 10$ kpc) or that the clouds are closer but with dust content less than ~ 0.3 times the local abundance.

The distances to the clouds are less constrained than the metallicity. Distance limits have been estimated by examining spectra of stars with known distance for absorption lines produced by intervening HVCs. The nondetection of absorption components led Danly et al. (1992) and de Boer et al. (1994) to conclude that complexes C and M lie at least 1.5 kpc from the plane. An upper limit to the distance of complex M was reported by Danly, Albert, & Kuntz (1993), who claim to have detected absorption toward a star at 4.4 kpc distance, thus bracketing the cloud to lie between 1.5 and 4.4 kpc from the plane of the Galaxy. This observation was recently confirmed by Keenan et al. (1995), who detected high-velocity Ca K line absorption toward the same star.

An observational clue to the HVC origin is provided by interferometer measurements of the 21 cm H I line (Schwarz, Sullivan, & Hulsbosch 1976; Schwarz & Oort 1981). Wakker & Schwarz (1991) mapped six HVC fields seen as large emission regions in single-dish observations. The fields include two regions in complex A (AIV.1 and AIV.2), one in complex M (M I.1), one in complex H, and two very high-velocity clouds. At 1′ resolution, they find several small clumps embedded in each of the larger emission regions. The clumps typically have sizes of $\sim 1'.5$–$5'$ and peak H I column densities $N \sim 1$–4×10^{20} cm^{-2}. The interferometer observations recover only $\sim 30\%$ of the single beam flux, similar to H I clouds in the Galactic plane. This, along with their line width results led Wakker & Schwarz to conclude that the HVCs have a multiphase structure consisting of a cold (30 K $\lesssim T \lesssim$ 300 K), dense ($n \sim 10$–100 cm^{-3}) core (analogous to the cold neutral medium in the disk, the CNM) and a warmer, more tenuous, halo (i.e., a warm neutral medium, the WNM).

Wakker & Schwarz (1991) also find an empirical relation between the CNM density n and cloud distance D by assuming that the depth of the clump is comparable to its projected size. For concentrations in complexes H and M with column density and angular size estimates classified as "good" or better (a total of 5 in H and 3 in M) they find $n = C/D$ cm^{-3}, with $C \approx 74 \pm 15$ and D measured in kiloparsecs. If the eight concentrations are at roughly the same distance, the results indicate that each clump has about the same average density. The field AIV.1 has only one observation of "good" quality with $C \approx 160$ while field AIV.2 shows a much wider range in densities than for H and M, with $C = 70$–200 (three clumps).

Wolfire et al. (1995, hereafter WHMTB) have developed a model for the multiphase equilibrium of the interstellar medium in which the CNM and WNM in the Galactic disk are heated by photoelectric emission from small grains and PAHs. Far-ultraviolet (FUV, $h\nu < 13.6$ eV) radiation, provided by OB stars and absorbed by dust grains, is converted to thermal energy in the gas with an efficiency of $\epsilon \sim 4\%$ in the CNM and $\epsilon \sim 1\%$ in the WNM. WHMTB demonstrate that this heating process can maintain the CNM and WNM in a stable thermal equilibrium at pressures comparable to those observed in the disk of the Galaxy (Jenkins, Jura, & Loewenstein 1983). In this paper, we apply the WHMTB models to HVCs in the Galactic halo. Using these models, along with the observed multiphase structure and metallicity constraints, we impose restrictions on the cloud distances and on models for the origin of the clouds.

In addition, observations of the soft X-ray background suggests that a hot ($T \sim 10^6$ K) ionized Galactic halo (HIM) may confine HVCs above the plane as initially proposed by Spitzer (1956). Simple fits to the X-ray observations indicate a local ($\lesssim 100$–200 pc) emission component with little or no extinction (a local "bubble") and an "absorbed" component which presumably arises in the halo (e.g., Garmire et al. 1992). *ROSAT* observations of X-ray shadows from high-latitude clouds (Snowden et al. 1991; Burrows & Mendenhall 1991; Lilienthal et al. 1992) and HVCs (Herbstmeier et al. 1995) provide direct evidence for X-ray emission from halo gas. The data are thus consistent with a multiphase structure of the Galactic corona consisting of two-phase (CNM + WNM) HVCs embedded in a hot ionized medium (HIM). We intend to use HVCs, in particular the two-phase structure, as probes of the density, temperature, and pressure of the corona (HIM).

We note that Ferrara & Field (1994) have recently proposed a method by which cloud distances might be determined by their Hα emission. Under isobaric conditions and for a range of possible halo pressure, they calculated the thermal and ionization structure of clouds exposed to the extragalactic Lyman continuum radiation field and halo emission. A relation was found between the column density at which clouds start to develop cold neutral cores and the cloud size. They propose that if this critical column could be measured, for example, by Hα emission, then cloud distances could be estimated by their observed angular size. Our method to constrain the distance to clouds is independent of and complementary to the Ferrara & Field (1994) method. They were mainly interested in the ionization structure in the outer $N \lesssim 10^{19}$ cm^{-2} of the cloud and made no allowance for the presence of a warm neutral phase. Our calculations, which include X-ray heating, cosmic-ray heating, and grain photoelectric heating, show that such warm neutral gas should exist over a wide range of conditions, which could make it difficult to apply their method in practice. In addition, we show how the distance to clouds may be constrained by measuring their shadows cast in the X-ray background.

We first discuss in § 2 the dominant thermal and ionization processes and present phase diagrams for HVCs for a range of heights above the Galactic plane. We construct a model for the halo pressure in § 3 using the observed emission measure of the HIM coupled with a realistic Galactic potential. We also discuss how the measurement of X-ray shadowing of HVCs can constrain their distance. In § 4 we show how the two-phase nature of HVCs can be used to constrain their distances and to discriminate among different models for their origin. A summary is presented in § 5.

2. MODEL CALCULATIONS

2.1. *Thermal and Ionization Balance in the Neutral Phases*

We calculate the thermal equilibrium temperature of a parcel of gas exposed to the Galactic cosmic-ray flux, the

Galactic radiation field, and the extragalactic radiation field (see WHMTB). Photoelectric heating from small grains and PAHs dominates the heating of the neutral phases provided the dust-to-gas ratio D/G is not too small. Bakes & Tielens (1994) have calculated the photoelectric heating rate for a size distribution of particles [$n(a)da \propto a^{-3.5}\,da$] extending from 100 to 3 Å in radius, and we have used their results here. Because the smallest particles (3–30 Å) dominate the photoelectric heating mechanism, the D/G ratios used in this paper refer to the mass of these particles per unit mass of gas. The heating efficiency is sensitive to the grain charge; thus, Bakes & Tielens (1994) calculated the charge distribution for each particle size taking into account photoionization, and electron and positive ion recombination. The resulting heating rate from the distribution of particles is given by

$$n\Gamma = 1.0 \times 10^{-24} n\epsilon G_0 \text{ ergs cm}^{-3}\text{ s}^{-1}\,, \quad (1)$$

where n is the density of hydrogen nuclei, $n = n(H^+) + n(H^0) + 2n(H_2)$, ϵ is the heating efficiency (fraction of FUV radiation absorbed by grains which is converted to gas heating), and G_0 is the incident FUV field normalized to Habing's (1968) estimate of the local interstellar value ($=1.6 \times 10^{-3}$ ergs cm^{-2} s^{-1}). A simple fit to ϵ given by Bakes & Tielens (1994) is

$$\epsilon = \frac{4.9 \times 10^{-2}}{1.0 + [(G_0\,T^{1/2}/n_e)/1925]^{0.73}} + \frac{3.7 \times 10^{-2}(T/10^4)^{0.7}}{1.0 + [(G_0\,T^{1/2}/n_e)/5000]}\,, \quad (2)$$

where T is the gas temperature and n_e the electron density.

The local FUV field in the Galactic plane as estimated by Draine (1978) is $\sim$1.7 times Habing's estimate (i.e., $G_0 \simeq 1.7$). Above the plane, however, the field is expected to be lower due to dust extinction from the disk, the lack of FUV sources from the (upper) 2π sr, and at great distances, due to the diminishing solid angle of the Galaxy itself. We shall first calculate the FUV intensity at the surface of the Galactic disk and then estimate the dependence on z height by assuming that the surface brightness of the Milky Way Galaxy scales with galactocentric radius like observed Sb galaxies. The total column density of hydrogen through the disk at the solar circle (excluding molecular gas, which has a negligible covering factor, and the HIM) is $\sim N \sim 8.7 \times 10^{20}$ cm^{-2} (Heiles 1976; Lockman 1984; Reynolds 1989) which gives an FUV optical depth (corrected for scattering) $\tau_{\rm FUV} \sim 0.8$ (Tielens & Hollenbach 1985). For a uniform layer of constant emissivity with this total optical depth, we find the intensity at the surface is a factor $\sim$0.6 times the midplane intensity. Thus, the FUV field at the surface of the disk amounts to $G_0 \sim 1.1$.

At height z above the plane, we assume the FUV field behaves as $G_0 = 1.1X(z)$, where the function $X(z)$ gives the height dependence. Hill et al. (1992) measured the total FUV disk flux $\mathscr{F}_D$ and FUV surface brightness profile $I_D(R)$ from the Sb galaxy M81 with results $\mathscr{F}_D = 3.9 \times 10^{-13}$ ergs cm^{-2} s^{-1} Å^{-1} and $I_D(R) = 1.7 \times 10^{-8}$ ergs cm^{-2} s^{-1} sr^{-1} Å^{-1} at $R = 8.5$ kpc from the center. The observations were conducted at a wavelength $\lambda = 1520$ Å using the Ultraviolet Imaging Telescope on board the *Astro-1* spacelab mission. Under the assumption that the radiation is emitted isotropically from the disk, the *mean* intensity at the disk surface is given by $I_D/2$ while the mean intensity at great distance z above the disk is given by $J_D(z) = \mathscr{F}_D(4\pi \cos i)^{-1}(d/z)^2$. The inclination angle to the disk is $i \sim 57°$ and the distance to M81 is $d \sim 3.3$ Mpc. A simple function which matches the mean intensity at the disk surface and at great distance is given by

$$J(z) = \frac{0.5I_D}{1 + 0.5I_D/J_D(z)}\,. \quad (3)$$

Assuming that the observed ratio of the disk intensity to total flux in M81 is similar to the Galaxy, we find

$$X(z) = \frac{1}{1 + (z/8.53\text{ kpc})^2}\,. \quad (4)$$

We compared this function with a numerical integration of the mean intensity above the disk of galaxy M81 using the observed surface intensity profile. Starting at the disk surface and at 8.5 kpc from the center, and proceeding to $z = 75$ kpc above the disk, we find equation (4) reproduces the numerical results to within $\sim$50%.

WHMTB find that although cosmic rays and X-rays never dominate the heating in the disk, they do set the level of ionization in the WNM and hence determine the heating efficiency of the grain photoelectric heating mechanism. In the CNM the electron density is set by the FUV ionization of metals (i.e., C^+). The ionization (and heating) due to soft X-rays is calculated using parameters consistent with the observed properties of the soft X-ray background (Garmire et al. 1992) and adjusted for positions above the gas disk. The total X-ray field is then a superposition of three components. The first component arises from extragalactic emission and consists of a power-law spectrum $I_\nu = 6.5 \times 10^{-19}\nu^{-0.4}$ ergs cm^{-2} s^{-1} sr^{-1} Hz^{-1} with a foreground absorption layer of column $N_{ex} = 3.9 \times 10^{20}$ cm^{-2} $- N(z)$, where the total column (3.9×10^{20} cm^{-2}) is from the Garmire et al. (1992) fit and where $N(z) = \int n(z)dz$ is the column from the midplane to z. We assume that $n(z)$ has a vertical distribution similar to the H I (WNM) distribution found by Dickey & Lockman (1990), i.e., $n(z)$ is given by a Gaussian $\propto \exp[-(z/318\text{ pc})^2]$ plus an exponential $\propto \exp(-z/403\text{ pc})$ with $N(z=0) = 0.0$ and $N(z=\infty) = 3.9 \times 10^{20}$ cm^{-2}. The second component, which presumably is produced in the Galactic halo, has gas at a single temperature $T_h = 2 \times 10^6$ K, emission measure $\text{EM}_h(z) = 2.5 \times 10^{-3}$ cm^{-6} pc, and intervening absorption layer of column $N_h(z) = 3.6 \times 10^{20} - N(z)$ cm^{-2}, where the temperature and total column (3.6×10^{20} cm^{-2}) are taken from the Garmire et al. (1992) fit. The last component is gas at a single temperature $T_{1b} = 10^{6.16}$ K, emission measure $\text{EM}_{1b}(z) = 5.3 \times 10^{-3}$ cm^{-6} pc, and intervening absorption layer $N(z)$ (local bubble component). Note that at $z = 0$ we recover the original fit by Garmire et al. (1992), and at heights $z \gtrsim 1$ kpc the local component is essentially removed due to extinction, leaving only the halo and extragalactic components. We also assume the X-rays are attenuated by a column N_w which accounts for absorption within the warm gas in the cloud. Columns much smaller than $\sim 10^{18}$ cm^{-2} would be substantially ionized by the Galactic and extragalactic X-ray radiation fields, while the peak clump (CNM) column densities are $\lesssim 4 \times 10^{20}$ cm^{-2}. We select a standard column of $N_w = 1 \times 10^{19}$ cm^{-2}. WHMTB demonstrated that for higher or lower columns (between 10^{18} cm^{-2} and 10^{20} cm^{-2}) the thermal pressure may vary by up to a factor of 3 from the $N_w = 10^{19}$ cm^{-2} case but is insensitive to N_w outside of this range.

We have included the effects of geometrical dilution at large z on the emission measures by multiplying $\text{EM}_h(z)$ and $\text{EM}_{1b}(z)$ by the function $X(z)$ (eq. [4]). For simplicity, we assume that the cosmic-ray intensity is also reduced by a factor

$X(z)$ above the plane. The primary cosmic-ray ionization rate is thus taken to be $\zeta = 1.8 \times 10^{-17} X(z)\ s^{-1}$ (McKee 1995).

WHMTB found that the dominant gas cooling process in the disk CNM is C II 158 μm fine-structure line emission. In the WNM several cooling processes contribute, including radiative line emission by Lyα and atomic metastable transitions, and electron recombination onto positively charged grains. Additional cooling is provided by the O I 63 μm fine-structure transition. The complete list of heating, cooling, and ionization processes is given in Table 1 of WHMTB.

2.2. *HVC Phase Diagrams*

The conditions under which an HVC may exist as a stable two-phase medium is investigated by the use of phase diagrams (thermal pressure P vs. hydrogen density n). A multiphase medium is possible when at fixed pressure nT, several solutions (n_i, T_i) of the thermal balance equation are possible. Not all solutions are stable, however. Thermal instability occurs for $d(\log P)/d(\log n) < 0$, while stable regions are indicated by $d(\log P)/d(\log n) > 0$. In general, the neutral atomic interstellar medium can maintain two stable phases at constant pressure in a range between a minimum pressure $P^{\rm min}$ and maximum pressure $P^{\rm max}$. The thermal pressure above the plane is determined by the temperature and density of the Galactic halo gas. Hence, HVCs may have a multiphase structure at a height z above the Galactic plane only if the halo pressure lies between $P^{\rm min}$ and $P^{\rm max}$; for halo pressure less than $P^{\rm min}$, only the warm phase is possible and for halo pressures greater than $P^{\rm max}$ only the cold phase is possible.

We present phase diagrams (thermal pressure P/k vs. density n) in Figures 1*a*–1*e* for five metallicities Z and dust-to-gas ratios D/G at several heights above the Galactic disk. The values of Z and D/G have been chosen to examine different models for the origin of HVCs. We measure Z and D/G relative to local interstellar values, with $Z = 1$ corresponding to the (solar system) elemental abundances of Anders & Grevesse (1989) (with the exception of O; see WHMTB) and *gas phase* abundances of $C/H = 3.0 \times 10^{-4}$ and $O/H = 4.6 \times 10^{-4}$. Recall that D/G refers to the mass of the small grain population. Our assumed grain size distribution implies that for $D/G = 1$, $\sim$4% of the cosmic carbon is in grains smaller than $\sim$15 Å.

Figure 1*a* shows the case for $Z = D/G = 1$, as appropriate for a Galactic fountain origin for HVCs with no small grain destruction. Near the Galactic disk (curve $z = 0$), two phases are possible between pressures $P^{\rm min}/k = 710$ K cm^{-3} and $P^{\rm max}/k = 2900$ K cm^{-3}. The region of thermal instability between densities $n \sim 0.5$ cm^{-3} and $n \sim 3.5$ cm^{-3} is a result of C II fine-structure line cooling which causes a rapid drop in temperature. At greater heights above the plane, both $P^{\rm min}$ and $P^{\rm max}$ drop due to diminished FUV flux (less grain photoelectric heating) and a lower rate of cosmic ray and soft X-ray ionization (reduced electron density and reduced heating efficiency).

Figure 1*b* shows results for $Z = 1$ and $D/G = 0.3$, as expected for a Galactic fountain origin for HVCs with moderate small grain destruction. If fountain gas is ejected at high velocity ($v \gtrsim 100$ km s^{-1}) from the Galactic disk, then grains can be destroyed in interstellar shocks with only a minor enhancement in the gas phase abundance of the dominant gas coolants (Jones et al. 1994). Decreasing the D/G ratio results in lower grain photoelectric heating. Hence, the temperature at a given density decreases and the curves shift to lower pressures. We note that it is somewhat uncertain whether small grains are depleted in the fountain model; the fast shocks will vaporize some dust but they will also shatter large dust particles to smaller grains.

Figures 1*c* and 1*d* show phase diagrams for stripped LMC gas. If HVCs are produced in this manner, then they should have dust and metal abundances similar to LMC gas; somewhat lower than Galactic abundances (e.g., Koornneef 1982; Dufour, Shields, & Talbot 1982; Russell & Bessell 1989). Figure 1*c* is for $D/G = Z = 0.3$ in which both the metallicity and dust abundance have been reduced by the same amount. Decreasing D/G and Z simultaneously results in a drop in both photoelectric heating and fine-structure line cooling and consequently, very similar temperatures and pressures compared to the $Z = D/G = 1$ case. Figure 1*d* illustrates the case for a moderate reduction in D/G and Z with $Z = 0.4$ and $D/G = 0.2$. These values are similar to LMC dust and metallicity (C) abundances as estimated by Koornneef (1982) and Russell & Dopita (1992). Phase diagrams for $Z = D/G = 0.01$ (primordial gas) are shown in Figure 1*e*.

2.3. *Thermal and Pressure Timescale*

Our model calculations assume sufficiently short cooling and expansion timescales that thermal and pressure balance is actually achieved. At a characteristic height $z \sim 3$ kpc, the WNM gas with low dust content ($D/G \sim 0.3$) is heated at a rate $\Gamma \simeq 7\text{–}9 \times 10^{-27}[(D/G)/0.3]$ ergs s^{-1} H^{-1} to a gas temperature $T \sim 8000$ K. Under isobaric conditions, the corresponding heating timescale is $t \sim 1\text{–}1.5 \times 10^{7}[(D/G)/0.3]^{-1}$ yr (see WHMTB, eq. [10]). The heating time in the CNM is considerably shorter.[4] Clouds with an average speed $v \sim 150$ km s^{-1} will have moved only $\sim$2 kpc during this time; provided the hot halo gas is in approximate pressure equilibrium, this leads to a variation in pressure by a factor $\lesssim$2. We also note that the thermal timescale is at least a factor $\sim$20 shorter than the travel time for clouds ram pressure stripped from the LMC at a distance of 65 kpc (Moore & Davis 1994). Therefore, thermal balance in the CNM and (marginally) in the WNM is achieved.

Pressure balance is also likely to be achieved. Wakker & van Woerden (1991) find a median cloud area of $\sim$3 deg^2. At a height of 3 kpc, the WNM cloud would be $\sim$50 pc in radius with a sound crossing time (to cloud center) of $t \sim 8 \times 10^6$ yr. The sound crossing time across the CNM is even shorter than the WNM. Thus, the time to achieve pressure equilibrium with the hot halo gas (assumed to be in approximate hydrostatic equilibrium) is relatively rapid compared to the time to experience a factor of 2 variation in the external pressure.

3. HOT HALO GAS

3.1. *Halo Pressure*

The thermal pressure in the Galactic halo determines whether an HVC could have a multiphase structure at a given height z. We consider an idealized halo which is isothermal and is in hydrostatic equilibrium in a realistic gravitational potential. The vertical component of Euler's equation for hydrostatic

[4] Galactic fountain gas with $D/G = 1$ has a heating rate a factor of $\sim$2 higher than the $D/G = Z = 0.3$ case, a rate somewhat lower than expected from the variation in D/G alone due to the effects of ion recombination on grains (see WHMTB). The $D/G = 1$ gas will have the highest heating//cooling rates and shortest equilibration times.

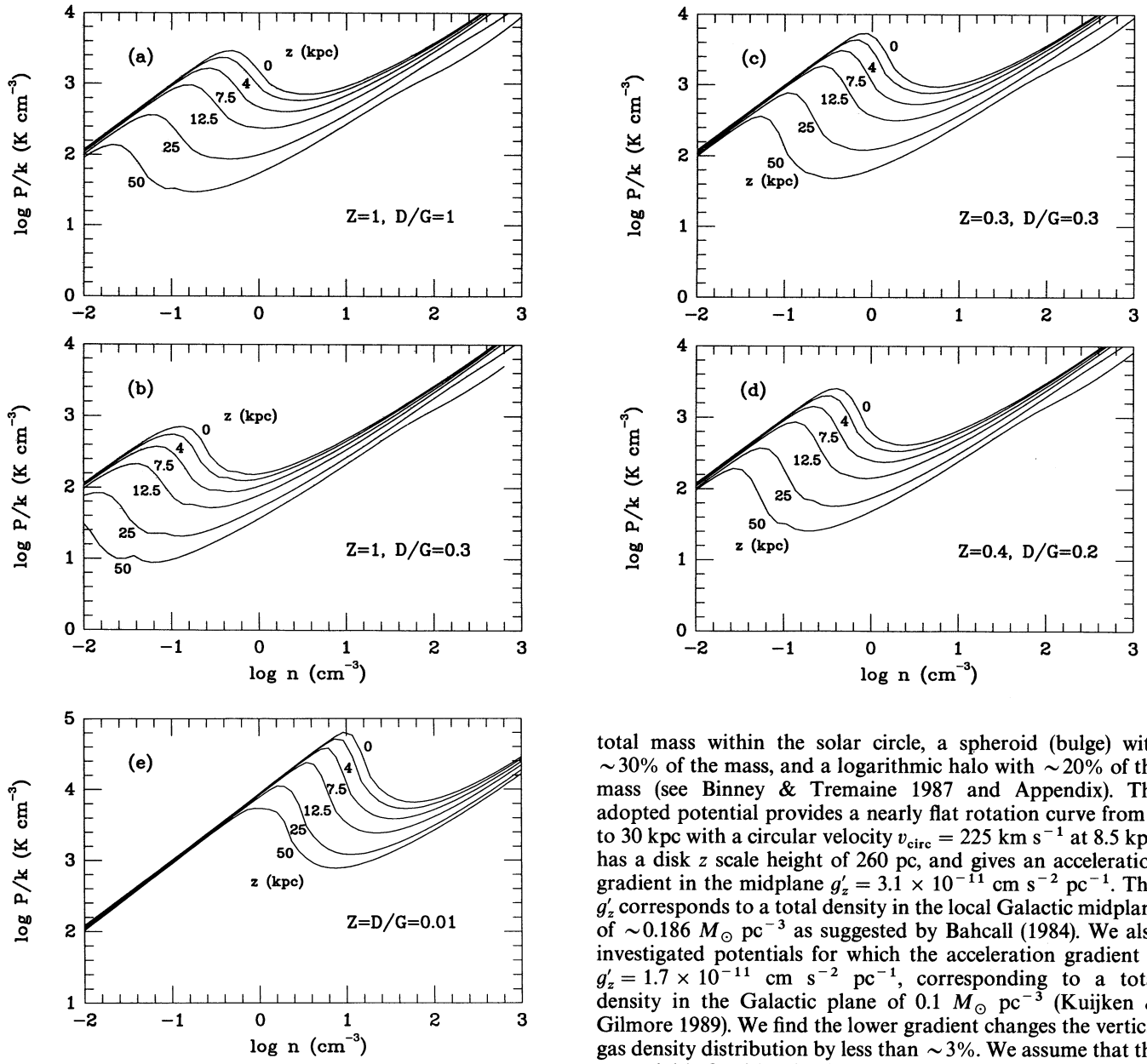

FIG. 1.—Thermal pressure P/k vs. hydrogen density n for various heights z above the Galactic plane. Panels show the effects of different dust-to-gas ratios, D/G, and metallicities Z relative to local abundances. (*a*) $Z = D/G = 1$ appropriate for a Galactic fountain origin for HVCs with no dust destruction. (*b*) $Z = 1$ and $D/G = 0.3$ appropriate for a Galactic fountain with moderate dust destruction. (*c*) $Z = D/G = 0.3$ appropriate for stripped LMC gas. (*d*) $Z = 0.4$, $D/G = 0.2$ appropriate for stripped LMC gas. (*e*) $Z = 0.01$, $D/G = 0.01$ appropriate for primordial gas.

equilibrium is independent of the rotation of the gas,

$$\frac{\partial}{\partial z}\,\phi(R, z) = -\frac{1}{\rho}\frac{\partial P}{\partial z}, \tag{5}$$

with ρ the gas density, $\phi(R, z)$ the Galactic gravitational potential as a function of galactocentric radius R and height z, and P the gas pressure. The gravitational potential is taken to be a sum of three components (Spergel 1994, private communication): a Miyamoto-Nagai disk with ~50% of the total mass within the solar circle, a spheroid (bulge) with ~30% of the mass, and a logarithmic halo with ~20% of the mass (see Binney & Tremaine 1987 and Appendix). The adopted potential provides a nearly flat rotation curve from 1 to 30 kpc with a circular velocity $v_{\rm circ} = 225$ km s^{-1} at 8.5 kpc, has a disk z scale height of 260 pc, and gives an acceleration gradient in the midplane $g'_z = 3.1 \times 10^{-11}$ cm s^{-2} pc^{-1}. This g'_z corresponds to a total density in the local Galactic midplane of ~0.186 $M_\odot$ pc^{-3} as suggested by Bahcall (1984). We also investigated potentials for which the acceleration gradient is $g'_z = 1.7 \times 10^{-11}$ cm s^{-2} pc^{-1}, corresponding to a total density in the Galactic plane of 0.1 $M_\odot$ pc^{-3} (Kuijken & Gilmore 1989). We find the lower gradient changes the vertical gas density distribution by less than ~3%. We assume that the potential is fixed by the distribution of stars plus dark matter so that equation (5) can be decoupled from Poisson's equation, i.e., the gravitational acceleration $g = \nabla\phi$ is not sensitive to the gas density distribution and temperature. For an isothermal, fully ionized halo, with sound speed $\sigma = 1.17 \times 10^2 T_6^{1/2}$ km s^{-1} ($T_6 = T/10^6$ K) and pressure $P = \rho\sigma^2$, the vertical density distribution in the solar circle has the solution

$$n(z, R) = n_0(R) e^{[\phi(R,0) - \phi(R,z)]/\sigma^2}, \tag{6}$$

with $n_0(R)$ and $\phi(R, 0)$ the density and potential in the midplane ($z = 0$), respectively. The midplane density is adjusted so that the total column matches the observed X-ray emission measure in the halo ($\mathrm{EM_h} = 2.5 \times 10^{-3}$ cm^{-6} pc; Garmire et al. 1992). The run of thermal pressure is then given by $P/k = 2.3n(z)T$, where the factor 2.3 is the number of particles (H^+, e^-, He^+, etc.) per hydrogen nucleus in a fully ionized gas. Figure 2 shows the results for isothermal halo temperatures $T_6 = 1$ and $T_6 = 2$. We find that the gas cooling time at these

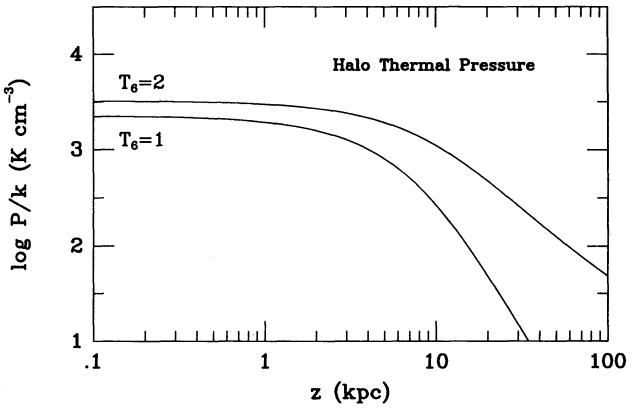

FIG. 2.—Thermal pressure P/k in the Galactic halo vs. height z. Curves are shown for an isothermal halo gas in hydrostatic equilibrium for temperatures 1×10^6 K ($T_6 = 1$) and 2×10^6 K ($T_6 = 2$). An analytic fit is given in eq. (7).

temperatures and densities is always much greater than the sound crossing time, and thus our assumption of hydrostatic equilibrium is justified. An analytic fit to the thermal pressure is given by

$$\frac{P}{k} = 2250 T_6^{1/2}\left(1.0 + \frac{z^2}{19.6}\right)^{-1.35/T_6} \text{ K cm}^{-3}, \qquad (7)$$

which matches the numerical results between 0 kpc $\leq z \leq$ 100 kpc to within $\sim$30% for $T_6 = 1$–2 and to within $\sim$50% for $0.5 \leq T_6 \leq 5$. Since our estimate of the halo pressure is based on local observations of the soft X-ray background, it is valid only at $R \sim 8.5$ kpc (although for arbitrary z). A global model for the halo must await a future paper.

The electrons in the hot halo gas make a nonnegligible contribution to the dispersion measure of pulsars far from the Galactic plane. The electron column density above height z, $N_{e\perp} = \int_z^\infty n_e dz'$, is shown in Figure 3 as a function of z for $T_6 = 1$ and 2. By comparison, the total value of $N_{e\perp}$ inferred from observations of pulsars in globular clusters is 7×10^{19} cm^{-2} (Reynolds 1991). Much of this column is presumably from 10^4 K gas, at $z < 1$ kpc, but Figure 3 shows that the HIM makes a significant contribution for pulsars with $z \gg 1$ kpc.

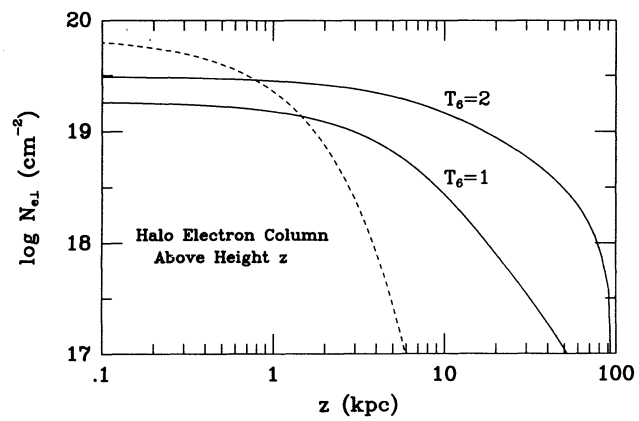

FIG. 3.—Electron column density $N_{e\perp}$ above height z perpendicular to the Galactic plane plotted as a function of z. Curves are shown for an isothermal halo gas in hydrostatic equilibrium (*solid*) for temperatures $T_6 = 1$ and $T_6 = 2$ ($T_6 = T/10^6$ K). Also shown is the electron column density using the electron distribution given by Reynolds (1991) inferred from observations of pulsars in globular clusters (*dashed line*).

With substantially more data on high z pulsars, it may be possible to provide direct evidence for—or against—a static, isothermal gaseous halo.

We note that the temperature used to calculate the halo density distribution may differ from that used to find the halo soft X-ray emission. Garmire et al. (1992) used an ionization equilibrium model to fit the observed broadband emission; recent spectral line observations, however, indicate that the HIM may not be in ionization equilibrium (Edgar et al. 1993). Thus we feel that we are justified in exploring a range of temperatures for the halo gas.

3.2. *X-Ray Shadowing by HVCs*

The discovery that individual neutral hydrogen clouds cast shadows in the soft X-ray background implies that HVCs can be used as probes for the structure of the halo gas. The results of a shadowing experiment provide an estimate of the emission produced in the foreground hot gas relative to the emission in the hot gas behind the cloud. With our adopted Galactic potential, we calculate the vertical density distribution and emission measure for different isothermal halo temperatures. Figure 4*a* shows the resulting ratio of the foreground emission measure $EM_{fg}(z)$ to total emission measure EM as a function of height z. We assume EM includes only the halo component ($EM = EM_h = 2.5 \times 10^{-3}$ cm^{-6} pc) and that $EM_{fg}(z)$ is the

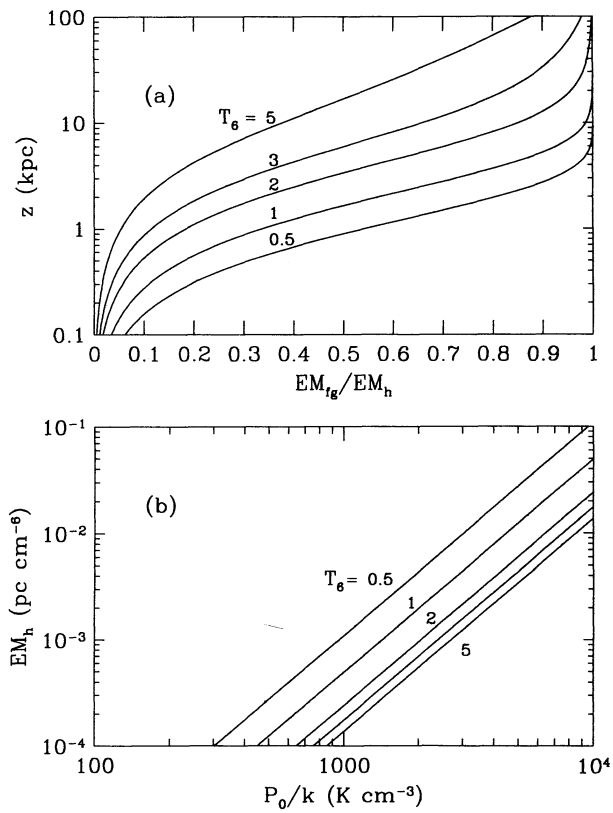

FIG. 4.—(*a*) HVC cloud height z vs. the fraction of halo emission measure which lies in front of the cloud (ratio of foreground emission measure to total emission measure) EM_{fg}/EM_h. Curves are shown for an isothermal halo gas in hydrostatic equilibrium for temperatures $T_6 = 0.5$, 1, 2, 3, and 5 ($T_6 = T/10^6$ K). These curves are appropriate for high-latitude lines of sight. (*b*) Halo emission measure EM_h as a function of thermal pressure in the Galactic midplane P_0/k. Curves are shown for an isothermal halo gas in hydrostatic equilibrium for temperatures $T_6 = 0.5$, 1, 2, 3, and 5 ($T_6 = T/10^6$ K).

integrated emission measure from height 0 to z. The extent of the halo gas will ultimately be limited by the intergalactic pressure. Here, we adopt a maximum extent of ~ 200 kpc. Our results are insensitive to the outer boundary for $T_6 \lesssim 3$. An observation will always include some contribution from the local bubble and extragalactic components. If these portions can be estimated and subtracted from the total, then the ratio EM_{fg}/EM_h (plotted in Fig. 4*a*), constrains the parameter space for the cloud height and halo temperature. Note that since we have used the emission measure and density distribution toward the Galactic pole, Figure 4*a* should not be used for low-latitude lines of sight.

As an example, we consider the results of Herbstmeier et al. (1995), who recently examined the *ROSAT* ($\frac{1}{4}$ keV) data toward complex M. Figure 4*a* should be applicable in this case since the observations are at high latitudes ($b \sim 50°$–$70°$). The analysis of the count rates are somewhat complicated by the fact that the halo emission toward the high-velocity gas is seen through a layer of low-velocity H I and the H II (Reynolds) layer. Herbstmeier et al. (1995) first obtained estimates of the local bubble component and halo component by fitting the soft X-ray background toward the low-velocity gas. Adopting an extragalactic background estimated by Snowden et al. (1994), they found $\sim 6.5 \times 10^{-4}$ counts s^{-1} arcmin^{-2} for the bubble and a variable halo with ~ 3–13×10^{-4} counts s^{-1} arcmin^{-2}. Fits toward the high-velocity gas indicated foreground halo emission at ~ 4–11×10^{-4} counts s^{-1} arcmin^{-2}. Thus, the range of observations result in only a minimum value for $EM_{fg}/EM_h \gtrsim 0.3$. We see in Figure 4*a* this ratio corresponds to a minimum height of greater than ~ 1 kpc for a $T_6 = 1$ halo or greater than ~ 2 kpc for a $T_6 = 3$ halo. The results are roughly consistent with the Danly et al. (1993) and Keenan et al. (1995) observations placing complex M between 1.5 and 4.4 kpc. Future observations interpreted with the aid of Figure 4*a* may further restrict these distances.

We also plot in Figure 4*b* the emission measure EM_h as a function of the thermal pressure in the midplane $P_0/k = 2.3 n_0 T$ for various halo temperatures. Since the emission measure is proportional to n_0^2, lines at constant temperature are simply given by $EM_h \propto (P_0/k)^2$. We note that Garmire et al. (1992) used Galactic metallicity to fit the observations and did not consider the thermal pressure in their fitting procedure. Nevertheless, we see that their emission measure provides reasonable results for the midplane pressure ($P_0/k \simeq 2000$–3000 K cm^{-3}) with $Z = 1$ and halo temperatures $T_6 = 1$–2. This is consistent with the results of Jenkins et al. (1987), who used observations of C I absorption lines to infer a median thermal pressure in the disk of $P_0/k \simeq 4000$ K cm^{-3}.

4. CONSTRAINING DISTANCES TO HVCs AND THEIR ORIGIN

4.1. *Distance to HVCs*

The empirical relation found by Wakker & Schwarz (1991) relating the HVC cloud distance and CNM density can be used to constrain the range of cloud heights for each class of models. We will adopt a slightly modified version of the Wakker & Schwarz (1991) relation by converting the distance D to height z above the Galactic plane using the relation $z = D \sin |b|$, with b the Galactic latitude of the cloud complex. Using the well determine measurements for complex M ($b = 67°$), we find that a cloud at height z kpc has a CNM density given by

$$n \simeq \frac{74 \pm 3}{fz} \text{ cm}^{-3}, \quad (8)$$

where f is the volume filling factor of dense gas observed with 1′ resolution (Wakker & Schwarz assumed $f = 1$). The concentrations in a single complex are presumably at the same height; complex A, however, may not be at the same height as M. Nevertheless, if the clumps in complex A are included in the $n - z$ relation we obtain nearly the same average CNM density as in equation (8), $n \simeq 80 \pm 26/fz$ cm^{-3}, which suggests that A may indeed be at a height similar to M. The larger range in estimated densities in A may be the result of substantially nonspherical concentrations or pressure variations within the complex. We have not included complex H since it lies nearly in the plane ($b = 1°$) and is not expected to be explained by the halo model we are constructing (e.g., vertical density distribution above the plane, FUV field above the plane, etc.).

The density n in equation (8) corresponds to a gas pressure P (from Fig. 1) which must lie between P^{min} and P^{max} (at height z) in order for the cloud to have two phases as observed. This means we can constrain the distance to the clouds to height z between z^{min} and z^{max}. If clouds were at $z < z^{min}$, the observed $n - z$ relation (eq. [8]) would imply high density and therefore pressures greater than P^{max} (i.e., only the cold phase would exist, contrary to observation). On the other hand, clouds at $z > z^{max}$ have low densities (eq. [8]), low pressures $P < P^{min}$, and only the warm phase would exist.

Adopting $f = 1$, we show in Figure 5 the run of cloud pressures P/k between distances, z^{min} to z^{max} for each model, for which two phases are possible. In Figure 5 we include, in addition to the thermal pressure of the halo, the ram pressure $P \simeq \rho v^2/2$ that HVCs are expected to experience due to their motion through the halo gas. (The factor $\frac{1}{2}$ is appropriate for clouds moving subsonically through an ambient medium, as can be seen from equation [122.2] in Landau & Lifshitz 1987). Results for the total pressure (thermal plus ram) are illustrated (*heavy solid line*) for an HVC infall speed of $v = 150$ km s^{-1} and for $T_6 = 1$, and $T_6 = 2$.

In general, we find that z^{max} is unconstrained by this method with the exception of the primordial case, for which $z^{max} \sim 2$ kpc. Therefore, the observed clouds could not be primordial unless they were at $z < 2$ kpc, which is contrary to observation (§ 1). This is not surprising, since the observed metallicity in

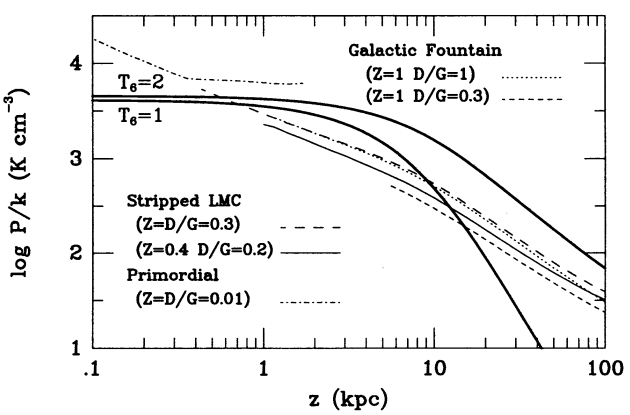

FIG. 5.—Cloud pressure P/k as a function of cloud height z. All curves (except heavy solid lines) assume the cloud (CNM) density is given by the $n - z$ relation (eq. [8]) with filling factor $f = 1$. Curves end where only one phase is possible. Results are shown for various dust-to-gas ratios, D/G, and metallicities Z as appropriate for different models for the origin of HVCs. Also plotted (*heavy solid lines*) is the sum of the ram pressure on an HVC for an average infall speed of $v \sim 150$ km s^{-1} plus the thermal halo pressure for gas temperatures of $T_6 = 1$ and $T_6 = 2$ ($T_6 = T/10^6$ K).

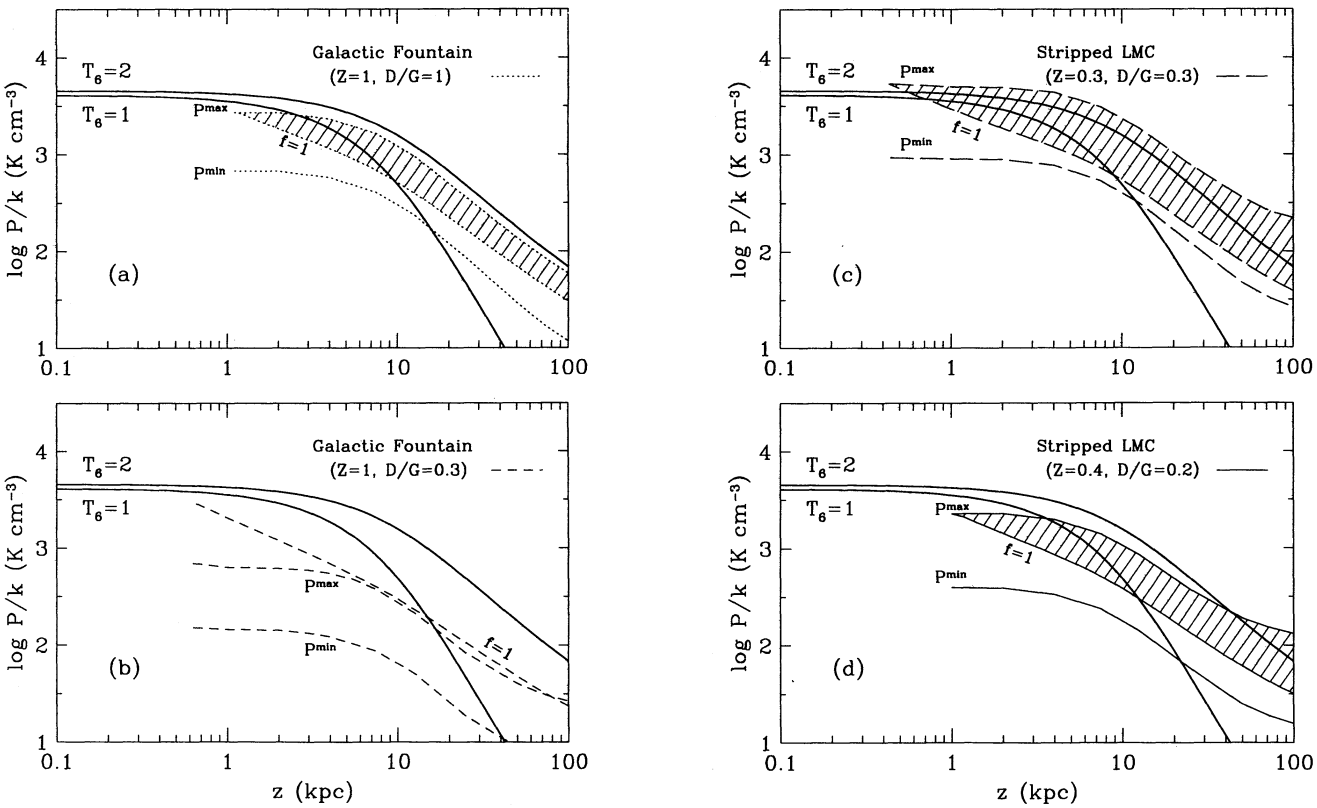

FIG. 6.—Range of cloud pressures for a two-phase equilibrium (P^{min} to P^{max}) as a function of cloud height z. Curves end where the $z - n$ relation (eq. [8] with $f = 1$) gives a solution for n where only one phase is possible. The shaded area shows the allowed cloud pressures for volume filling factors less than unity (eq. [8] with $f \leq 1$). Also plotted is the sum of the ram pressure on an HVC for an an average infall speed of $v \sim 150$ km s^{-1} plus the thermal halo pressure for gas temperatures of $T_6 = 1$ and $T_6 = 2$ ($T_6 = T/10^6$ K). (*a*) $Z = D/G = 1$ appropriate for a Galactic fountain origin for HVCs with no dust destruction. (*b*) $Z = 1$ and $D/G = 0.3$ appropriate for a Galactic fountain with moderate dust destruction. The curves have been extended to low values of z to show the trends of the P^{max}, P^{min}, and $f = 1$ results. (*c*) $Z = D/G = 0.3$ appropriate for stripped LMC gas. (*d*) $Z = 0.4$, $D/G = 0.2$ appropriate for stripped LMC gas. (*e*) $Z = 0.01$, $D/G = 0.01$ appropriate for primordial gas.

some of the clouds rules out a primordial origin. The remaining models have z^{min} ranging from ~ 1 kpc to ~ 5 kpc and thus produce two-phase solutions over a plausible range of cloud heights. In the most restrictive case, i.e., if the $n - z$ relation is valid, if the filling factor f equals one, and if the pressure on the clouds is given by the heavy solid lines, then consistent solutions occur only at the intersection of the heavy lines (thermal halo pressure plus ram pressure) and the lighter solid or broken lines (cloud pressure). However, we show below how relaxing, for example, the $f = 1$ assumption modifies the range of consistent solutions.

Figures 6*a*–6*e* show separately the pressure curves of Figure 5 with P^{min} and P^{max} added. These figures illustrate the maximum possible effects of filling factors less than unity on the inferred P/k values. A value for $f < 1$ would result in higher CNM densities and thus higher HVC pressures. At a given z the pressure could increase to a maximum of P^{max}, at which point the two-phase structure is no longer possible. We have shaded in the region between the standard relation (eq. [8] with $f = 1$) and P^{max} to illustrate a plausible range of two-phase solutions. (We note that the Galactic fountain model $Z = 1$, $D/G = 0.3$ is only marginally acceptable for z greater than 5.5 kpc since P exceeds P^{max} by $\sim 10\%$–20%. Since a slight increase in D/G could increase P^{max}, we have retained this model for discussion. The curves have been extended to low values of z to show the trends of the P^{max}, P^{min}, and $f = 1$ results). Typically $f \sim 0.2$–0.4 is required for $P = P^{max}$ for the stripped LMC gas and standard dust Galactic fountain cases. It is clear that with filling factors less than unity, either stripped LMC gas or Galactic fountain gas may produce two-phase clouds (over a wide range of heights) which are confined by the halo pressure. For the cases shown in Figures 6*a*, 6*b*, and 6*d*, there is evidence that a $T_6 = 1$ halo is preferred to a $T_6 = 2$ halo.

4.2. *Origins of HVCs*

Our models show that a multiphase cloud structure can exist within a range of heights above the Galactic plane. This range,

especially the minimum height, is sensitive to the metallicity and dust abundance. We summarize in this section the constraints imposed by our results on the various theories for the origin of HVCs. For comparison, a thorough discussion of the *dynamical* constraints on the origin of HVCs is given by Wakker & Bregman in Wakker (1989, chap. 5) and Wakker (1991a). As they point out, a single model may not be able to account for all the HVCs; in particular, Galactic models are unable to account for clouds at high Galactic latitudes ($b > 45°$) or very high velocity clouds, those with $|v_{lsr}| > 200$ km s^{-1}. On the other hand, infall models (gas stripped from the LMC) exhibit these attributes but do not produce the observed distribution of flux at lower velocities as well as the Galactic models. We note, however, that the Wakker & Bregman models did not account for the dynamical (drag) effects of the halo gas with column densities comparable to the HVC column densities.

4.2.1. *Galactic Fountain Origin*

In a Galactic fountain, hot gas produced by supernovae rises out of the disk, cools, and falls back into the disk (Shapiro & Field 1976; Bregman 1980). Isolated supernovae are unable to break out of the disk (McKee & Ostriker 1977), but superbubbles powered by sufficiently large associations can (Heiles 1990). Wakker & Bregman (Wakker 1989, chap. 5) have shown that a Galactic fountain naturally accounts for many of the features of HVCs with $|v_{lsr}| < 200$ km s^{-1}. In their model, only $\sim 10\%$ of the gas in the fountain is observable at velocities $|v_{lsr}| > 100$ km s^{-1}. Allowing for this lower velocity gas associated with the fountain, they infer a mass flow of 5 $M_\odot$ yr^{-1} onto the disk, a value that is consistent with observations of hot gas in the halo (McKee 1993).

A prediction of the fountain model is that the velocity distribution of the HVCs should join smoothly onto the distribution of H I at lower velocities, since all the H I in the Galaxy is believed to be energized by supernovae (Spitzer 1977; McKee & Ostriker 1977). Kulkarni & Fich (1985) have shown that the H I near the north Galactic pole (NGP) and the south Galactic pole has a smooth velocity distribution extending beyond 100 km s^{-1}, although they regarded the data above 80 km s^{-1} as being of questionable accuracy. After removing the effects of the infalling gas in the NGP region, they estimated that 1% of the gas has $|v_{lsr}| > 100$ km s^{-1}. By using Wakker's (1991b) results to evaluate the mean H I column density $\langle N_{HVC} \rangle = \int N_{HVC} dC$ where N_{HVC} is the column density with $|v_{lsr}| > 100$ km s^{-1} and dC is the fraction of the sky covered by gas in the range of column density dN_{HVC}, we find that the mean column density of HVCs, averaged over the sky, is $\langle N_{HVC} \rangle = 1.7 \times 10^{18}$ cm^{-2}. This is indeed $\sim 1\%$ of the H I column measured out of the Galactic plane (Kulkarni & Fich 1985), thereby confirming their earlier estimate. If the HVCs do not have a Galactic origin, then in principle they could have produced a feature in the H I velocity distribution at high velocities. The fact that they do not is consistent with a fountain origin.

What constraints can our results place on fountain models? The Galactic fountain model with $Z = D/G = 1$ has a minimum height $z^{min} \sim 1$ kpc, consistent with the available distance determinations. However, the lack of 100 μm infrared emission from dust indicates that either D/G is less than 0.3 for nearby clouds, or that $D/G = 1$, but clouds are more distant than ~ 10 kpc (Wakker & Boulanger 1986). Here, however, D/G refers to the 100 μm emitting dust, which is likely to be particle sizes $\gtrsim 100$ Å. If clouds were indeed ejected from the plane to such large heights, then we expect that a considerable amount of dust would be destroyed by shocks, although the resultant size distribution of the dust is not clear. Thus, we argue that Galactic fountain models with $Z = 1$ must also have $D/G < 1$.

Fountain models require that the gas be heated to at least 10^6 K (Wakker & Bregman in Wakker 1989, chap. 5), which requires a shock velocity of at least 270 km s^{-1}. Calculations of grain destruction discussed by Seab (1987) show that grains smaller than ~ 100 Å may be destroyed by thermal sputtering in such nonradiative shocks. To model this case, we have $Z = 1$, $D/G = 0.3$. As seen in Figure 6*b*, this model is problematic since two phases exist only for $z \gtrsim 5$ kpc. Clouds closer than 5 kpc could exist only as cold cores, a result inconsistent with the distance estimates and interferometer observations. We also find an implausibly tight set of constraints on this model. First, the filling factor f may not be much less than one, since lower values of f lead to cloud pressures greater than P^{max}. Second, we find a halo pressure which falls in the range between P^{min} and P^{max} only for $z \gtrsim 15$ kpc and $T_6 \gtrsim 1$. Therefore, the $Z = 1$, $D/G = 0.3$ fountain model is difficult to reconcile with observations. The $Z = 1$, $D/G = 1$ model provides an acceptable match, but seems to be in confict with the Wakker & Boulanger (1986) observations. One possibility is that the fast shock might shatter enough large grains to maintain $D/G = 1$ for the small (~ 15 Å) particles, but still reduce the 100 μm emitting grains by a factor of 3. If this is the case, then we would predict for normal near-infrared colors (Boulanger & Pérault 1988) a 12 μm intensity of ~ 0.1 MJy sr^{-1} from the HVC cores. Typically, the residuals left by zodiacal light subtraction at 12 μm are of this same order. Since the *IRAS* beam size is comparable to the core size of these HVCs, this emission will be difficult to detect. *Infrared Space Observatory* (*ISO*), however, with its smaller beam may have a better chance for success.

The largest uncertainty in constraining the origin models and halo parameters has been the distance ambiguity. What conclusions can be drawn if we *assume* that the average cloud height is $z \approx 3$ kpc as inferred from the Danly et al. (1993) observations? The Galactic fountain model with $Z = D/G = 1$ (Fig. 6*a*) is ruled out by the Wakker & Boulanger (1986) limits on the dust content of such clouds if the dust size distribution extends continuously from large ($\gtrsim 100$ Å) to small (~ 3 Å) grain sizes. The Galactic fountain model with $Z = 1$, $D/G = 0.3$ has $z^{min} = 5$ kpc and does not allow multiphase clouds at $z = 3$ kpc. Our results thus indicate that one can reconcile the Galactic fountain model with two-phase HVCs 3 kpc above the plane only with a dust size distribution which is sharply peaked at small sizes.

4.2.2. *Primordial Origin*

We note that primordial models have $z^{max} \sim 2$ kpc (Fig. 6*e*), which conflict with most distance determinations to HVCs. These models can also be ruled out by the existing absorption line observations, which show the presence of a significant amount of metals in each case (see § 1).

4.2.3. *Stripped LMC Origin*

Models with $Z < 1$, corresponding to stripped LMC gas, have $z^{min} \sim 0.5$ kpc for $Z = D/G = 0.3$ and $z^{min} \sim 1$ kpc for $Z = 0.4$, $D/G = 0.2$. Both models provide z^{min} and D/G within the observational constraints. We must now consider the addi-

tional constraints imposed by the halo pressure. For $Z = 0.4$, $D/G = 0.2$ models (Fig. 6*d*) we find that if $f = 1$, then a two-phase cloud is in pressure equilibrium with a $T_6 = 1$ isothermal halo at a height $z \sim 10$ kpc from the plane. Smaller filling factors imply higher CNM densities and pressures. Thus, at a given height, f could decrease with a corresponding increase in the pressure until the cloud P reached a maximum of P^{max}. Using P^{max} as the upper limit to the cloud pressure yields a range of possible cloud heights from 4 kpc $< z <$ 10 kpc in a $T_6 = 1$ halo. For clouds to exist at 4 kpc, the filling factor must be $f \sim 0.3$.

Models for $Z = D/G = 0.3$ (Fig. 6*c*) show a wide range in heights for which two phases are possible. For $f = 1$ we find clouds in equilibrium with the $T_6 = 1$ halo at distances of both $z \sim 10$ kpc *and* $z \sim 0.8$ kpc. Filling factors less than 1 (~ 0.5) allow for two-phase clouds at all intermediate heights. If pressures are as large as P^{max} then multiphase clouds could exist only for $T_6 \gtrsim 2$. For a $T_6 = 2$ halo, all distances $z > 0.7$ kpc are possible for filling factors between $f \sim 1$ and $f \sim 0.2$. However, in general, $T_6 = 2$ halos are less conducive to two-phase HVCs, as seen in Figures 6*a*–6*d*. At these high temperatures, the halo pressure drops slowly with z, and the enhanced pressure eliminates the low-density phase.

Assuming a height of 3 kpc for the stripped LMC gas with $Z = 0.4$ and $D/G = 0.2$ (Fig. 6*d*) implies $f < 1$ and $T_6 \lesssim 1$. This gas satisfies the *IRAS* constraints but can have two phases for only a narrow range in f near $f \sim 0.4$; values of f much greater would imply halo temperatures $T_6 < 1$, while values of f much smaller would imply CNM pressures greater than P^{max}. Finally, stripped LMC models with $Z = D/G = 0.3$ (Fig. 6*c*) easily produce two-phase clouds at $z = 3$ kpc. Clouds are confined by the $T_6 = 1$ halo for filling factors $f = 0.5$ and by the $T_6 = 2$ halo for filling factors $f = 0.3$.

We note that a search for H I absorption in the Magellanic Stream revealed no cold cores (Mebold et al. 1991). Figures 6*c* and 6*d* show that the $T_6 = 1$ halo pressure drops below P^{min} at distances of 10–20 kpc. The $T_6 = 2$ halo produces either two-phase clouds or cold cores at all distances. Thus, no cold cores are expected to be found in a $T_6 = 1$ halo at distances greater than $z \gtrsim 20$ kpc.

5. SUMMARY

We have calculated the thermal equilibrium gas temperature and constructed phase diagrams for high-velocity clouds in the Galactic halo. Our method uses the results of Bakes & Tielens (1994) to find the photoelectric heating from small grains and PAHs and explicitly includes the heating and ionization due to the diffuse soft X-ray background and due to cosmic rays. Two stable phases of the neutral gas exist between a narrow range of pressures, with P^{min} and P^{max} decreasing with height above the Galactic plane. We calculate the pressure in the halo gas and compare with the pressures required for two-phase clouds. The observed existence of two phases sets constraints on the distance to the HVCs and their metallicity and thus their origin.

Using a realistic Galactic potential and normalizing to the observed emission measure in the diffuse "absorbed" soft X-ray component, we find that a halo with $T = 10^6$ K will produce the measured thermal pressure in the midplane. We present results for the shadowing produced by HVCs in this halo component and discuss how the shadowing can provide distance estimates to the HVCs. The electrons in the hot gaseous halo may be detectable through their contribution to the dispersion measure of pulsars far from the Galactic plane.

We find that consistent two-phase models can be constructed with a range of heights above the Galactic plane. The range is sensitive to the metallicity and dust abundance. For extremely low metallicities, such as would exist in primordial clouds falling toward the plane, the two phases exist only at $z < 2$ kpc, contrary to most measured distance lower limits to HVCs. A primordial origin for HVCs is also directly ruled out in some cases where the metal abundances have been constrained to lie between $0.2 < Z < 1$. For this range of metallicities, which encompass Galactic Fountain clouds as well as stripped LMC clouds, the *minimum height* is sensitive to the value of Z and the dust abundance.

Observations of the dust-to-gas ratio (*IRAS* 100 μm emission; Wakker & Boulanger 1986) rule out nearby ($z \lesssim 10$ kpc) clouds with standard abundances of 100 μm emitting grains ($a \sim 100$ Å). More distant Galactic clouds satisfy this constraint but would have significant dust destruction due to the shocks that lofted the clouds so far from the plane. Our fountain model with $D/G = 0.3$ and $Z = 1$ shows that the observed two-phase clouds must be at least 5 kpc from the plane, which is marginally inconsistent with the limit of 4.5 kpc for complex M set by Danly et al. (1993). Closer clouds could exist only as cold cores. A fountain model with $D/G = 1$ provides a much more satisfactory fit. Since D/G refers to the 3–30 Å grains which dominate the photoelectric heating, we can reconcile our results with the Wakker & Boulanger observations only if large dust is preferentially shattered and destroyed. For this $D/G = 1$ case, we predict a 12 μm intensity of ~ 0.1 MJy sr^{-1} from the HVC cores.

The stripped LMC models do not require a modified grain size distribution. Two-phase clouds in pressure equilibrium with a hot $T_6 = 1$–2 Galactic corona are possible over a wide range in distance. Our curves indicate, however, that for clouds to exist at distances less than 10 kpc, the volume filling factors in the observed HVCs must be less than 1, with $f \sim 0.2$–0.5. We predict that no cold cores are expected to be found at distances greater than $z \gtrsim 20$ kpc in a $T_6 = 1$ halo. This result is consistent with the lack of cold cores seen in the Magellanic Stream if the Stream distance is greater than 20 kpc.

Additional crucial observations are needed. In particular, observations of the cloud metallicity directly constrain the origin of HVCs independent of our theoretical results. In Galactic fountain models, clouds move outward in Galactocentric radius and therefore should always have a metallicity at least equal to that of the local interstellar gas. In contrast, gas stripped from the LMC should have somewhat lower metallicity. In addition, observations of the dust content and the gas filling factor in the cold cores would constrain our models. More X-ray shadowing experiments would also be valuable.

We would like to thank R. Gerber and T. Steiman-Cameron for useful discussions and comments. We also thank an anonymous referee for several helpful suggestions. This research was initiated while M. G. W. was supported by the National Academy of Sciences through an NRC postdoctoral fellowship and completed with support from NSF grant AST 92-21289 and a NASA Theory Program grant 399-20-10-12. Primary support for C. F. M. was provided from NSF grant AST 92-21289. Theoretical studies of interstellar dust at NASA Ames are supported under task 399-20-01-30 through NASA's Theory Program.

APPENDIX

GALACTIC POTENTIAL

The halo density distribution is calculated using a simple Galactic potential provided by Spergel (1994, private communication), modified for a finite halo mass. The potential is constructed from three axisymmetric components in cylindrical (R, z) coordinates: (1) A Miyamoto-Nagai disk potential

$$\phi_1(R, z) = -\frac{C_1 v_{\rm circ}^2}{[R^2 + (a_1 + \sqrt{z^2 + b_1^2})^2]^{1/2}}, \tag{A1}$$

with constants $C_1 = 8.887$ kpc, $v_{\rm circ} = 225$ km s^{-1}, $a_1 = 6.5$ kpc, and $b_1 = 0.26$ kpc; (2) a spherical (bulge) potential

$$\phi_2(R, z) = -\frac{C_2 v_{\rm circ}^2}{a_2 + \sqrt{z^2 + R^2}}, \tag{A2}$$

with constants $C_2 = 3.0$ kpc, and $a_2 = 0.70$ kpc; and (3) a logarithmic halo

$$\phi_3(R, z) = C_3 v_{\rm circ}^2 \ln(a_3^2 + R^2 + z^2), \tag{A3}$$

with constants $C_3 = 0.325$, and $a_3 = 12$ kpc. The total potential is then given by the sum of the three components $\phi(R, z) = \phi_1(R, z) + \phi_2(R, z) + \phi_3(R, z)$. In this form, the potential is divergent at infinity. In reality, the halo mass distribution is finite and ϕ_3 will change form at sufficiently large distances. Generalizing the potential used by Lin et al. (1995), we write

$$\phi_3(R, z) = C_3 v_{\rm circ}^2 \ln\left\{\frac{[1 + (a_3^2 + R^2 + z^2)/r_h^2]^{1/2} - 1}{[1 + (a_3^2 + R^2 + z^2)/r_h^2]^{1/2} + 1}\right\}, \tag{A4}$$

which corresponds to a mass distribution

$$M_3(r) = \frac{2C_3 v_{\rm circ}^2 r^3}{G(a_3^2 + r^2)[1 + (a_3^2 + r^2)/r_h^2]^{1/2}} \tag{A5}$$

where $r^2 = R^2 + z^2$. For their standard model, Lin et al. (1995) adopt $r_h = 210$ kpc, far larger than the distances relevant to this paper. With this form of the potential, we can determine the minimum pressure in the intergalactic medium required to confine the gaseous halo,

$$P_{\rm IGM} > 2.3n(R, \infty)kT = P_0(R)e^{\phi(R,0)/\sigma^2} \tag{A6}$$

(c.f., Ferrera & Field 1994). Using the total potential with ϕ_3 given by equation (A4) we have $\phi(R = 8.5$ kpc, $0) = -1.68 \times 10^5$ (km s^{-1})^2. From Figure 4b with $T_6 = 1$ and EM$_h = 2.5 \times 10^{-3}$ pc cm^{-6} the thermal pressure in the midplane is $P_0/k \simeq 2300$ K cm^{-3} and we find $P_{\rm IGM}/k > 1 \times 10^{-2}$ K cm^{-3}.

The z-component of the gravitational acceleration is related to the potential by $g_z = -\partial\phi(R, z)/\partial z$. For $r \ll r_h$, the potential terms (A1)–(A3) yield:

$$g_{z,1} = -\frac{C_1 v_{\rm circ}^2 z(1 + a_1/\sqrt{z^2 + b_1^2})}{[R^2 + (a_1 + \sqrt{z^2 + b_1^2})^2]^{3/2}}, \tag{A7}$$

$$g_{z,2} = -\frac{C_2 v_{\rm circ}^2 z}{(a_2 + \sqrt{z^2 + R^2})^2(z^2 + R^2)^{1/2}}, \tag{A8}$$

$$g_{z,3} = -\frac{2C_3 v_{\rm circ}^2 z}{(a_3^2 + R^2 + z^2)}. \tag{A9}$$

REFERENCES

Anders, E., & Grevesse, N. 1989, Geochim. Cosmochim. Acta, 53, 197
Bahcall, J. N. 1984, ApJ, 276, 169
Bajaja, E., et al. 1985, ApJS, 58, 143
Bakes, E. L. O., & Tielens, A. G. G. M. 1994, ApJ, 427, 822
Binney, J., & Tremaine, S. 1987, Galactic Dynamics (Princeton: Princeton Univ. Press)
Boulanger, F., & Pérault, M. 1988, ApJ, 330, 964
Bowen, D. V., & Blades, J. C. 1993, ApJ, 403, L55
Bregman, J. N. 1980, ApJ, 236, 577
Burrows, D. N., & Mendenhall, J. A. 1991, Nature, 351, 629
Corbelli, E., & Salpeter, E. E. 1988, ApJ, 326, 551
Danly, L., Albert, C. E., & Kuntz, K. D. 1993, ApJ, L29
Danly, L., Lockman, F. J., Meade, M. R., & Savage, B. D. 1992, ApJS, 81, 125
de Boer, K. S., Altan, A. Z., Bomans, D. J., Lilienthal, D., Moehler, S., van Woerden, H. Wakker, B. P., & Bregman, J. N. 1994, A&A, 286, 925
Dickey, J. M., & Lockman, F. J. 1990, ARA&A, 28, 215
Draine, B. T. 1978, ApJS, 36, 595
Dufour, R., Shields, G., & Talbot, R. J. 1982, ApJ, 252, 461
Edgar, R. J., Sanders, W. T., Juda, M., Kraushaar, W. L., & McCammon, D. 1993, BAAS, 25, 805
Ferrara, A., & Field, G. B. 1994, ApJ, 423, 665
Garmire, G. P., Nousek, J. A., Apparao, K. M. V., Burrows, D. N., Fink, R. L., & Kraft, R. P., 1992, ApJ, 399, 694
Giovanelli, R. 1980, AJ, 85, 1155
———. 1981, AJ, 86, 1468
Habing, H. J. 1966, Bull. Astron. Inst. Netherlands, 18, 323
———. 1968, Bull. Astron. Inst. Netherlands, 19, 421
Heiles, C. 1976, ApJ, 204, 379
———. 1990, ApJ, 354, 483
Herbstmeier, U., Mebold, U., Snowden, S. L., Hartmann, D., Burton, W. B., Moritz, P., Kalberla, P. M. W., & Egger, R. 1995, A&A, 298, 606
Hill, J. K., et al. 1992, ApJ, L37

Houck, J. C., & Bregman, J. N. 1990, ApJ, 352, 506
Hulsbosch, A. N. M., & Wakker, B. P. 1988, A&AS, 75, 191
Jenkins, E. B., Jura, M., & Loewenstein, M. 1983, ApJ, 270, 88
Jones, A., Tielens, A. G. G. M., Hollenbach, D. J., & McKee, C. F. 1994, ApJ, 433, 797
Keenan, F. P., Shaw, C. R., Bates, B., Dufton, P. L., & Kemp, S. N. 1995, MNRAS, 272, 599
Kepner, M. E. 1970, A&A, 5, 444
Koornneef, J. 1982, A&A, 107, 247
Kuijken, K., & Gilmore, G. 1989, MNRAS, 239, 651
Kulkarni, S. R., & Fich, M. 1985, ApJ, 289, 792
Landau, L. D., & Lifshitz, E. M. 1987, Fluid Mechanics (New York: Pergamon)
Li, F., & Ikeuchi, S. 1992, ApJ, 390, 405
Lilienthal, D., Hirth, W., Mebold, U., & de Boer, K. S. 1992, A&A, 255, 323
Lin, D. N. C., Jones, B. F., & Klemola, A. R. 1995, ApJ, 439, 652
Lockman, F. J. 1984, ApJ, 283, 90
Lu, L., Savage, B. D., & Sembach,K. R. 1994a, ApJ, 426, 563
———. 1994b, ApJ, 437, L119
Lynden-Bell, D. 1976, MNRAS, 174, 695
Mathewson, D. S., Cleary, M. N., & Murray, J. D. 1974, ApJ, 190, 291
McKee, C. F. 1993, in Back to the Galaxy, ed. S. S. Holt & F. Verter (New York: AIP), 499
———. 1995, in preparation
McKee, C. F., & Ostriker, J. P. 1977, ApJ, 218, 148
Mebold, U., Greisen, E. W., Wilson, W., Haynes, R. F., Herbstmeier, U., & Kalberla, P. M. W. 1991, A&A, 251, L1
Meyer, D. M., & Roth, K. C. 1991, ApJ, 383, L41
Moore, B., & Davis, M. 1994, MNRAS, 270, 209
Murai, T., & Fujimoto, M. 1980, PASJ, 32, 581
Oort, J. H. 1966, Bull. Astron. Inst. Netherlands, 18, 421
———. 1970, A&A, 7, 381
Reynolds, R. J. 1989, ApJ, 339, L29
———. 1991, in The Interstellar Disk-Halo Connection in Galaxies, ed. H. Bloemen (Dordrecht: Kluwer), 67
Robertson, J. G., Morton, D. C., Schwarz, U. J., van Woerden, H., & Murray, J. D. 1991, MNRAS, 248, 508
Rosen, A., & Bregman, J. N. 1995, ApJ, 440, 634
Russell, S. C., & Bessell, M. S. 1989, ApJS, 70, 865
Russell, S. C., & Dopita, M. A. 1992, ApJ, 384, 508
Savage, B. D., et al. 1993, ApJ, 413, 116
Savage, B. D., & de Boer, K. S. 1979, ApJ, 230, L77
———. 1981, ApJ, 243, 460
Schwarz, U. J., & Oort, J. H. 1981, A&A, 101, 305
Schwarz, U. J., Sullivan, W. T., & Hulsbosch, A. N. M. 1976, A&A, 52, 133
Seab, C. G. 1987, in Interstellar Process, ed. D. Hollenbach & H. A. Thronson, Jr. (Dordrecht: Reidel), 491
Sembach, K. R., Savage, B. D., Lu, L., & Murphy, E. M. 1995, ApJ, 451, 616
Shapiro, P. R., & Field, G. B. 1976, ApJ, 205, 762
Snowden, S. L., Hasinger, G., Jahoda, K., Lockman, F. J., McCammon, D., & Sanders, W. T. 1994, ApJ, 430, 601
Snowden, S. L., Mebold, U., Hirth, W., Herbstmeier, U., & Schmitt, J. H. M. M. 1991, Science, 252, 1529
Spitzer, L. 1956, ApJ, 124, 20
———. 1977, Physical Processes in the Interstellar Medium (New York: Wiley)
Tielens, A. G. G. M., & Hollenbach, D. 1985, ApJ, 291, 722
Wakker, B. P. 1989, Ph.D. thesis, Groningen University
———. 1991a, The Interstellar Disk-Halo Connection in Galaxies, ed. H. Bloemen (Dordrecht: Kluwer), 27
———. 1991b, A&A, 250, 499
Wakker, B. P., & Boulanger, F. 1986, A&A, 170, 84
Wakker, B. P., & Schwarz, U. J. 1991, A&A, 250, 484
Wakker, B. P., & van Woerden, H. 1991, A&A, 250, 509
West, K. A., Pettini, M., Penston, M. V., Blades, J. C., & Morton, D. C. 1985, MNRAS, 215, 481
Wolfire, M. G., Hollenbach, D., McKee, C. F., Tielens, A. G. G. M., & Bakes, E. L. O. 1995, ApJ, 443, 152 (WHMTB)